DOI:10.1190/1.1885613

3-D converted-wave processing: Wind River Basin case history

Richard R. Van Dok, James E. Gaiser, Alexander R. Jackson, Western Geophysical, Denver, Colorado, and Heloise B. Lynn, Lynn Incorporated; Houston, Texas*

Summary

Renewed interest in processing and interpretation of P to S converted-wave (P-S) seismic data over the past few years can be attributed partially to new analysis and processing techniques that have produced successful results when applied to 3-D surveys (Garotta and Granger, 1988; Harrison, 1992). Concepts originally developed and implemented for 2-D surveys are now being extended to 3-D, giving rise to new challenges in both processing and interpretation. We present a processing case study of one such 3-D survey in the Wind River Basin in Wyoming. Key steps discussed include surface-consistent deconvolution, surface-consistent statics, common conversion-point (CCP) binning, azimuth limiting, layer stripping and Alford rotation.

Introduction

We present a case history in a known gas field located in Wyoming's Wind River Basin. The target objective is a sequence of thin layers of shales, silts, and sands, interspersed with several thin coal units in a lower Tertiary formation at 1,500-3,000 m in depth. A 3-D three-component seismic survey was acquired during the fall of 1995 covering approximately 5 square km over this field. The objective of the survey was to identify naturally fractured tight gas sands within this formation, exploiting the azimuthal anisotropy previously identified in the area (Lynn, et al., 1996). This study is part of an ongoing project dedicated to the detection of naturally fractured tight gas reservoirs funded by the U.S. Department of Energy, Morgantown Energy Technology Center.

Acquisition Parameters

The seismic survey consisted of 458 3-component receiver locations arranged in 9 parallel lines and held static throughout the acquisition. The inline spacing was 67 m and the receiver line spacing was 201 m covering approximately 5 square km (Figure 1). Each receiver location consisted of 12 buried 3-C geophones arranged in a 6-9 m circular array. The geophones were oriented such that one of the horizontal phones was exactly east-west (H1) and the other north-south (H2). Buried dynamite charges of 9 kg each at a depth of 20 m were distributed as evenly as possible over the 5 square km survey area. One result from this acquisition layout is a wide distribution in source to receiver azimuths and offsets necessary for interpreting P-S wave data.

Preprocessing

Source and receiver location information was calculated and confirmed for all three components. Once the coordinate information was in place and initial bad trace editing was completed, the three components were separated into individual volumes for processing. The data recorded on the vertical phones were then processed using standard 3-D P-wave methods. Key steps included refraction statics, reflection statics, surface-consistent deconvolution, DMO, and time migration. After statics were resolved, the data were separated into two limited-azimuth volumes (N90E/N270E and N0E/N180E, +/- 45 degrees) for subsequent processing and interpretation (Lynn, et al., 1996).

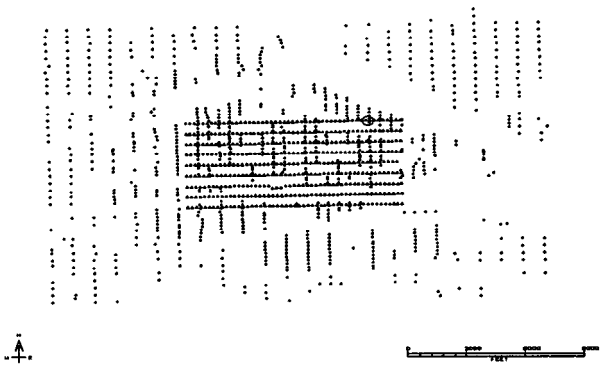

Figure 1. Surface source and receiver location map. Source lines are oriented north-south, receiver lines are oriented east-west. Source location for Figure 2 located in upper right corner of receiver patch denoted by an open circle. Map scale is approximately 1:120,000.

After the P-wave data were completed, both the H1 and H2 data volumes were processed as similarly as possible in order to preserve relative amplitude and phase characteristics. Relative amplitudes were preserved by applying a single geometrical spreading correction function followed by a time- and offset-variant scalar function (Figure 2). The same scalars were applied to both volumes. Noisy traces were reduced using an automatic trace editing algorithm. Coherent noise energy due to ground roll was attenuated using an adaptive *f-x* technique that models the noise and subtracts it from the records (Gaiser, 1994). While both of these noise-attenuation techniques are adaptive, potentially affecting the two components differently, it was observed that by choosing the parameters carefully and restricting the action of each algorithm the positive benefits outweighed any potential degradation.

Surface-Consistent Deconvolution

Due to the asymmetric raypaths associated with P-S data and potentially different responses present in a converted-wave survey between the sources and receivers, the deconvolution process was divided into two steps. The fist step involved the application of the

DOI:10.1190/1.1885613

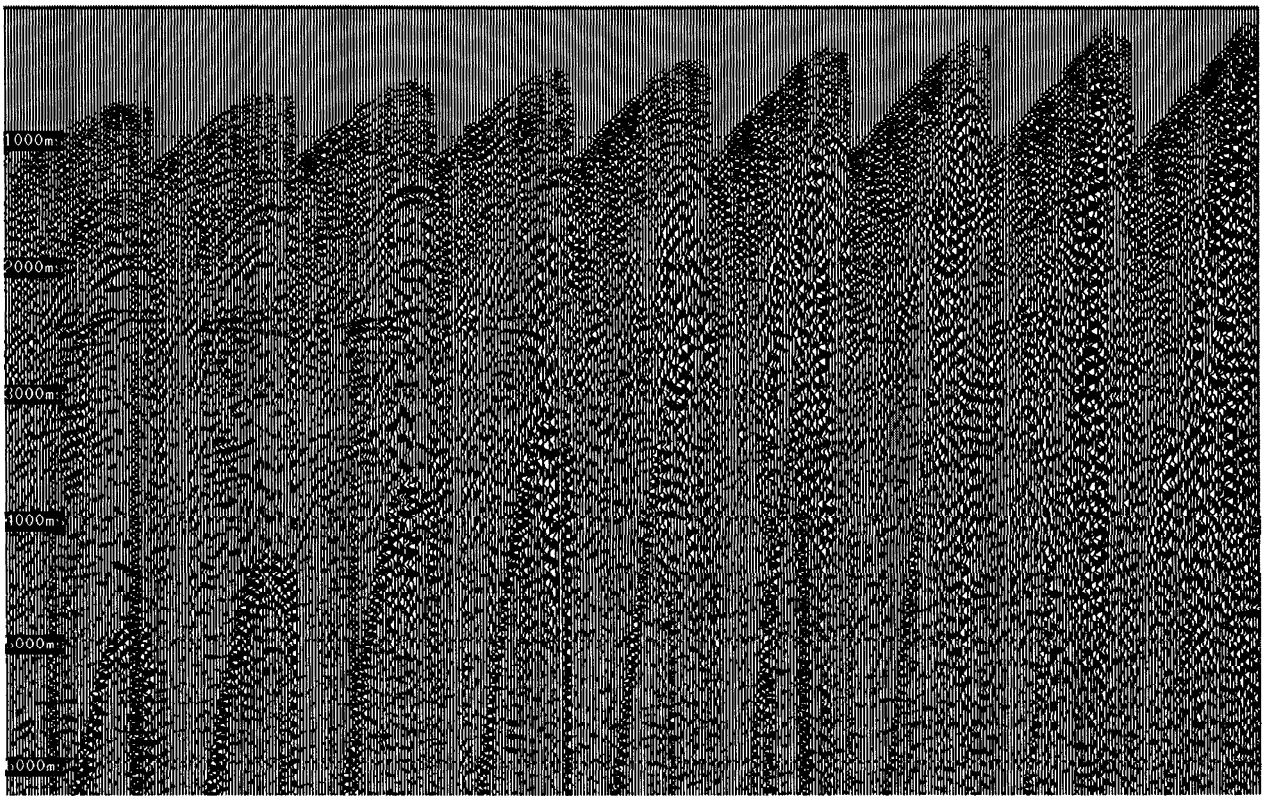

Figure 2. Typical shot record (H1 geophone). Note converted-wave reflections at 2.4 seconds.

source deconvolution operator calculated during the P-wave processing flow. Second, the receiver and offset terms for the deconvolution were computed from the P-S wave data. Source-receiver azimuths parallel (+/- 22.5 degrees) to the respective geophone directions were selected and combined for the computation of the deconvolution operators. The chosen directions provided the best signal-to-noise ratio for the spectral analysis. A single operator was then calculated for each station location and offset in the survey and applied to both the H1 and H2 data. Evaluating the H1 and H2 data simultaneously improved the statistics for the spectral analysis and surface- consistent decomposition, stabilized the phase characteristics across the survey, and maintained the polarization relationship of shear waves on the two receiver components

Surface-Consistent Statics

As was the case with deconvolution, calculation and application of static shifts were separated into two steps. Source statics from the P-wave processing were first applied to the P-S data. Residual reflection statics were then calculated for the P-S data. Both source and receiver residual statics were calculated using a maximum shift of 64 msec. Reflection statics, velocity analyses, and common conversion-point binning (detailed below) were iterated twice to allow for convergence of the statics and velocities. For the same propagation direction, differences in the optimum computed statics for the Hl and H2 receivers were observed, possibly due to near-surface anisotropy. Bates et al. (1996) documented in field data within this survey the 2-4% S-wave birefringence of the top 20 m and the S1 (fast S-wave) orientation as N90E/N270E. In order to achieve the best coherency in each stack volume, the second iteration of residual statics was independently performed on each azimuth volume (detailed below) and receiver component. Again, it was observed that producing a more coherent image on all volumes and possibly compensating for near-surface anisotropy was beneficial and any differential timing shifts introduced by separate static solutions did not affect the overall time structure.

Common Conversion-Point Binning

One of the most important steps in P-S processing is the proper positioning of the true reflection point for any source and receiver combination. Because of the asymmetry of the P-S raypath, a midpoint coordinate transform must be applied. The movement from geometric midpoint (CMP) to common conversion-point (CCP) depends on the velocity of the medium as well as the source and receiver position (Tessmer and Behle, 1988). Our approach uses the P-wave velocities previously interpreted in conjunction with the derived P-S velocities and is implemented over user-defined windows. As stated earlier, two iteration sequences were utilized for

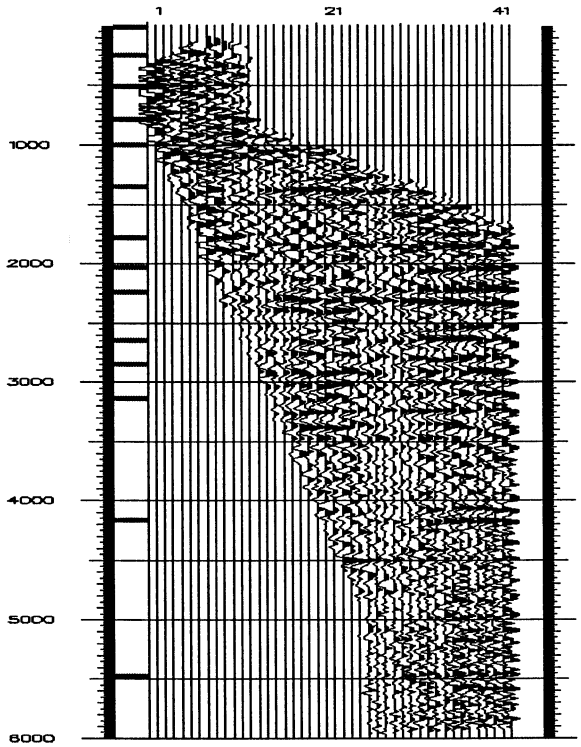

Figure 3. Common-conversion point supergather for the H1 geophone with statics, NMO, and mute applied. Trace spacing is 33 m and the propagation direction is N90E/N270E.

this survey. The initial transformation of the CMP to CCP was done using one window over the entire data trace. Once the coordinates were recalculated, the data were binned and sorted into their new CCP locations. After picking velocities and statics, the original data were rebinned using the newly interpreted P-S velocities and three windows centered on key horizons. DMO algorithms are another effective method for achieving this coordinate transform but can be expensive to run and typically do not preserve surface-consistent static information. Ideally, velocity and statics are resolved using the iteration sequence described above prior to the application of DMO.

NMO, Mute and Stack

Standard velocity analyses were used to interpret stacking velocities for both the H1 and H2 data after each iteration of statics and CCP binning. In general, the H1 data quality was much better than the H2, for any given propagation direction. The very best data quality was the H1 data set in the east-west direction (N90E/N270E). A first-arrival mute was selected from normal-moveout corrected gathers. An inside mute, also selected from the gathers, was used to remove the noisy near offsets, over which the P-S energy ranged from very weak to nonexistent. After CCP binning, normal-moveout, and muting (Figure 3), the data were stacked to produce a single output trace for every bin.

Azimuth Limitation

Given the wide source-receiver azimuth distribution for this survey, it was necessary to create limited- azimuth volumes for many of the processing steps as well as the final interpretable products. From previous studies (Lynn et al., 1996) and this survey's P-wave processing, the primary direction of azimuthal anisotropy was estimated as due east-west (N90E/N270E). This direction also corresponded, in general, to the best quality data recorded into the H1 geophones. Azimuth slices were selected for both the H1 and H2 data (Figures 4 and 5) in the east-west direction (+/- 22.5 degrees). Azimuths perpendicular (north-south, NOE/N180E) were also selected for both H1 and H2 to create four volumes for subsequent layer stripping and Alford rotation. A simple, but easily overlooked step required before stacking data within an azimuth volume was the reversal of polarity for negative source-receiver offsets due to the nature of reflected shear waves and the orientation of the horizontal geophones in front of and behind the source. The selection of which direction to reverse was arbitrary but remained consistent for all volumes. Due to the rectangular nature of the acquisition layout and the azimuth and offset distribution, two additional directions, N45E/N225E and N135E/N315E, were also chosen as final products. The fold distribution, overall data quality, and imaged area for these two directions were more alike than for the east-west and north-south volumes.

Time Migration

Random noise attenuation was applied to each volume followed by a bandpass filter to precondition the data for migration. Conventional 3-D time migration was performed for each azimuth volume using a full 3-D *f-k* algorithm. The velocity used was a single P-S velocity function, chosen as an average over the survey area.

Alford Rotation and Layer Stripping

Azimuthally selected data that propagate in orthogonal directions provided the four horizontal components for the Alford rotation and layer stripping. In this case, data propagating in the N45E/N225E (+/- 22.5 degrees) and N135E/N315E (+/- 22.5 degrees) directions each resulted in H1 and H2 components that were rotated into radial and transverse components. Principal symmetry axes were determined by finding the orientation that minimized reflection energy on the transverse components and the percent azimuthal anisotropy was determined from time aligning the resulting radial components. Results at locations supported by good data quality showed variations in percent azimuthal anisotropy ranging from 0-10 % with principal axes varying both spatially and temporally.

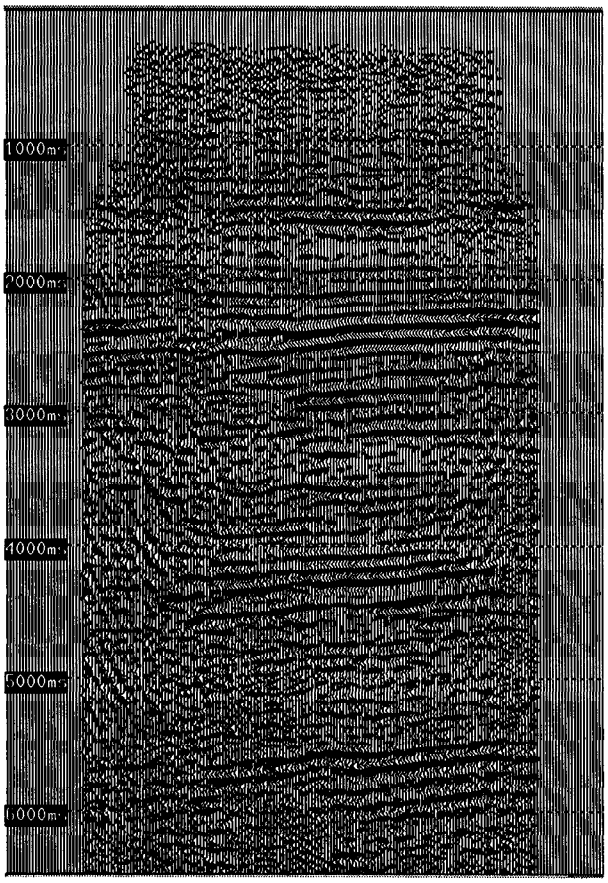

Figure 4. Final east-west stack with random noise attenuation and 8-24 Hz band-pass filter (H1 geophone, N90E/N270E azimuths).

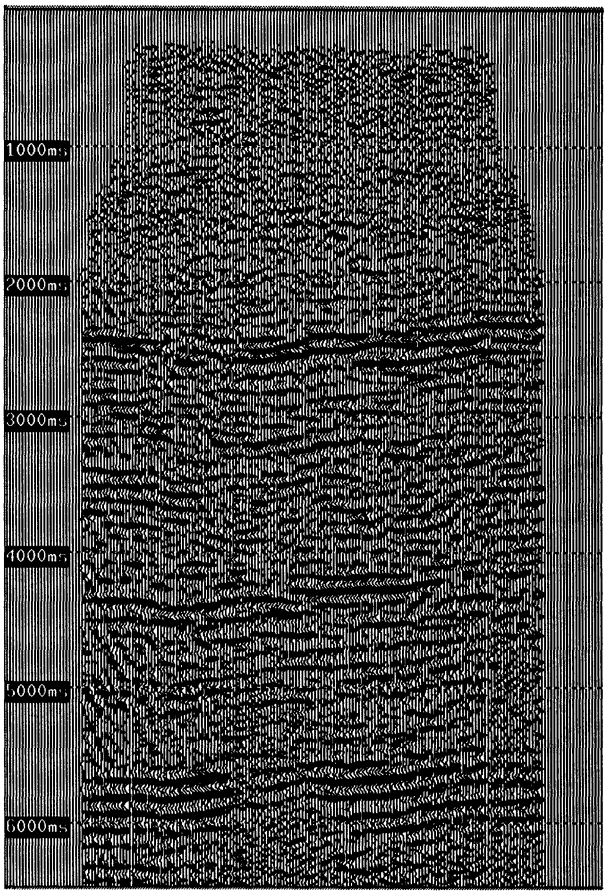

Figure 5. Final east-west stack with random noise attenuation and 8-24 Hz band-pass filter (H2 geophone, N90E/N270E azimuths).

Conclusions

Effective 3-D converted-wave processing may be accomplished using conventional seismic processing algorithms with the addition of a few select programs, such as CCP binning, Alford rotation, and layer stripping. Surface-consistent processing methodologies developed for land 3-D P-wave data may be adapted to P-S wave data by properly separating the source and receiver terms and attempting to preserve relative variations in amplitudes and travel times between the two horizontal components. By limiting source to receiver propagation azimuths, multiple data volumes may be obtained for subsequent Alford rotation, layer stripping and anisotropy analysis. Data shown here, while varying in quality throughout the survey area, demonstrates the success of many of these methodologies while producing interpretable results for further anisotropy evaluation.

References

Bates, C.R., Phillips, D., Lavely, E., 1996, Near surface variability in shear-wave velocity anisotropy: *66th Ann. Internat. Mtg., Soc. Expl. Geophys., Expanded Abstracts,* p. 739-742.

Gaiser, J.E., 1995, 3-D prestack f-x coherent noise suppression: *65th Ann. Internat. Mtg., Soc. Expl. Geophys., Expanded Abstracts,* p. 1354-1357.

Garotta, R.J., and Granger, P.Y., 1988, Acquisition and processing of 3-C X 3-D data using converted waves: *58th Ann. Internat. Mtg., Soc. Expl. Geophys., Expanded Abstracts,* p. 995-997.

Harrison, M.P., 1992, Processing of P-SV surface seismic data: anisotropy analysis, dip moveout, and migration: Ph.D. dissertation, University of Calgary.

Lynn, H.B., Simon, M.K., Bates, C.R., Van Dok, R.R., 1996, Azimuthal anisotropy in P-wave 3-D (multi-azimuth) data: *The Leading Edge,* 15, p. 923-928.

Tessmer, G. and Behle, A. 1988, Common reflection point data-stacking technique for converted waves: *Geophysical Prospecting,* 36, p. 671-688.